Surface Science 603 (2009) 455–461

Contents lists available at ScienceDirect

Surface Science

journal homepage: www.elsevier.com/locate/susc

An IRAS study of CO bonding on Sn/Pt(1 1 1) surface alloys at maximal pressures of 10 Torr

Adrian Hightower [a,*], M. Dolores Perez [b], Bruce E. Koel [c]

[a] Occidental College, Physics, 1600 Campus Road, Los Angeles, CA 90041, USA
[b] University of Southern California, Los Angeles, CA 90089, USA
[c] Lehigh University, Bethlehem, PA 18015, USA

ARTICLE INFO

Article history:
Received 9 September 2008
Accepted for publication 21 November 2008
Available online 3 December 2008

Keywords:
Carbon-monoxide
Pt(1 1 1)
Platinum
Catalyst
Pt_3Sn
Sn–Pt alloy
FTIR
IRAS

ABSTRACT

The adsorption of CO on Pt(1 1 1), (2 × 2) and ($\sqrt{3} \times \sqrt{3}$)*R*30° Sn/Pt(1 1 1) surface alloys has been studied using temperature programmed desorption (TPD), low energy electron diffraction (LEED) and infrared reflection adsorption spectroscopy (IRAS). The presence of Sn in the surface layer of Pt(1 1 1) reduces the binding energy of CO by a few kcal/mol. IRAS data show two C–O stretching frequencies, ~2100 and ~1860 cm^{-1}, corresponding to atop and bridge bonded species, respectively. Bridge bonded stretching frequencies are only observed for Pt(1 1 1) and (2 × 2) Sn/Pt(1 1 1) alloy surfaces. A slight coverage dependence of the vibrational frequencies is observed for the three surfaces. High pressure IRAS experiments over a broad temperature range show no indication of bridge bonded CO on any of the three surfaces. Direct CO adsorption on Sn sites is not observed over the measured temperature and pressure ranges.

1. Introduction

The wide use of bimetallic catalysts has motivated extensive studies of well-defined surface alloys [1–3]. In particular, CO has been widely studied on bimetallic platinum surfaces as a prototypical molecule to investigate the influence of site-blocking and electronic phenomena on reaction kinetics [4–9]. There is also special interest in CO behavior as a poison and/or intermediate in the mechanism of low temperature hydrocarbon oxidation [10–13]. The drive to better correlate the performance of bimetallic heterogeneous catalysts with ultrahigh vacuum (UHV) surface science studies has lead to numerous high pressure surface studies on single crystals [14–18]. This work presents results of high pressure vibrational studies of CO on Sn/Pt(1 1 1) alloys to better understand the so-called "pressure-gap".

Sn/Pt(1 1 1) alloys are known to form two ordered surfaces, (2 × 2) Sn/Pt(1 1 1) and ($\sqrt{3} \times \sqrt{3}$)*R*30° Sn/Pt(1 1 1) by vapor deposition of Sn on Pt(1 1 1) single crystals followed by careful annealing under high vacuum conditions [5,19]. Low energy ion scattering spectroscopy (LEISS) and depth profiling by Auger electron spectroscopy (AES) indicate this procedure yields surface alloys with Sn atoms localized to the top two surface layers [20]. Fig. 1 displays the proposed alloy surfaces and corresponding LEED patterns. Sn atoms protrude 0.02 nm above the surface-Pt plane for both surfaces [21]. For the (2 × 2) structure, pure-Pt threefold sites are present, but no adjacent pure-Pt threefold sites exist. All pure-Pt threefold sites are eliminated in ($\sqrt{3} \times \sqrt{3}$)*R*30° structure. For brevity throughout this paper, (2 × 2) Sn/Pt(1 1 1) and ($\sqrt{3} \times \sqrt{3}$)*R*30° Sn/Pt(1 1 1) surface alloys will be referred as (2 × 2) and $\sqrt{3}$ alloys, respectively.

The bonding and structure of CO on clean Pt(1 1 1) has been well-studied by TPD and high resolution electron energy loss spectroscopy (HREELS). CO is chemisorbed perpendicular to the surface with carbon bonding directly to metal atoms. CO initially populates atop sites at low coverage and then populates bridges sites form a *c*(4 × 2) structure at θ_{CO} = 0.5 (θ_{CO} is defined as the ratio of CO molecules to surface atoms) [22,23]. These results have been supported by density-functional theory (DFT) calculations [24,25]. Dense CO adlayers forming "linear domain-wall" *c*($\sqrt{3} \times 7$) structures at θ_{CO} = 0.71 coverage have also been reported on Pt(1 1 1) [26].

A thorough inspection of the CO adsorption on these alloy surfaces concluded that alloying with Sn causes only slight decreases in the CO binding energy to the surface compared to Pt(1 1 1) [4]. At low temperatures (~100 K) and saturation coverage, CO was found to chemisorb to atop and bridge sites on the Pt(1 1 1), (2 × 2) and $\sqrt{3}$ surfaces. Xu et al. proved the existence of a modifier precursor state and used this to explain how Sn influences CO chemisorption kinetics in a manner other than that predicted by a

* Corresponding author. Tel.: +1 323 259 2826; fax: +1 323 341 4858.
E-mail address: hightower@oxy.edu (A. Hightower).

0039-6028/$ - see front matter © 2008 Elsevier B.V. All rights reserved.
doi:10.1016/j.susc.2008.11.020

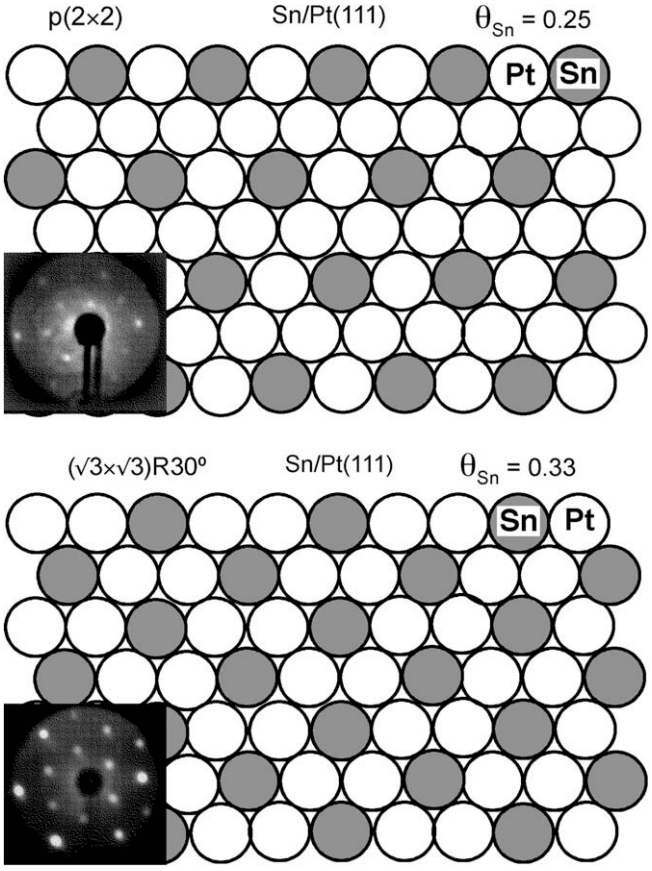

Fig. 1. Schematics diagrams and corresponding LEED patterns of the two ordered Sn/Pt(1 1 1) surface alloys that were investigated.

simple site-blocking model [5]. Previous LEED studies report a $(2\sqrt{3} \times 2\sqrt{3})R30^\circ$ structure for CO adlayers at saturation coverage on the (2×2) surface while no ordered CO adlayers were observed on the $\sqrt{3}$ surface [4]. The same study utilized HREELS to observe CO populating both atop and bridge sites for Pt(1 1 1), (2×2) and $\sqrt{3}$ alloy surfaces at saturation coverage. Yet the limited resolution of HREELS measurements leaves questions regarding the coordination of CO relative to Sn sites on surface alloys.

Recent surface studies and DFT calculations on the (1 1 1) surface of bulk Pt_3Sn alloys have provided valuable insight into the activity of CO oxidation on Pt–Sn surfaces [27,28]. HREELS studies by Dupont et al. [9] on the (2×2) $Pt_3Sn(1\,1\,1)$ bulk alloy surface have found CO populating both atop and bridge sites similar to the HREELS measurements on the (2×2) surface alloy [4]. High pressure polarization modulation infrared reflection absorption spectroscopy (PM-IRRAS) studies on $Pt_3Sn(1\,1\,1)$ bulk alloys exposed to CO followed by O_2 at room temperature found more efficient CO desorption from the $(\sqrt{3} \times \sqrt{3})R30^\circ$ surface than from the (2×2) [18]. It is important to note that surface studies on bulk alloy must contend with segregation of Sn to the surface [29]. In contrast, the surface alloys studied in this work are extremely thin (less than two monolayers) and are thought to be less susceptible to surface segregation. Indeed an important advantage of studying surface alloys over bulk alloy surfaces is the opportunity to exploit Gibbsian surface segregation to achieve a desired surface rather than fight against it [30].

In the present work we use infrared reflection adsorption spectroscopy (IRAS) to gain further insight on the interaction of CO on two ordered Sn/Pt(1 1 1) surface alloys. The high resolution of infrared (IR) spectroscopy makes it well-suited to study the C–O stretching modes of CO on Pt surfaces [31]. Care must be taken when using IRAS to assign CO populations to atop, bridge, and threefold hollow sites of Pt(1 1 1). Dynamic dipole–dipole coupling in dense CO adlayers is known to influence IRAS spectra by "intensity transfer" phenomena by which higher frequency bands gain intensity at the expense of lower frequency bands [32]. Nevertheless, the high resolution of IRAS measurements should provide insight into the interaction of CO and Sn on alloy surfaces.

Here we present IRAS studies at varying CO coverage on the Pt(1 1 1) and two alloys surfaces at pressures ranging from 10^{-10} to 10 Torr. Despite background features in the high pressures IRAS spectra, we can draw some conclusions on CO adsorption and packing on the Pt(1 1 1), (2×2) and $\sqrt{3}$ surfaces.

2. Experimental methods

Experiments were performed in a stainless steel UHV chamber equipped for Auger electron spectroscopy (AES), low energy electron diffraction (LEED), temperature programmed desorption (TPD) and Fourier-transform infrared (FTIR) spectroscopy. The chamber had a base pressure of 2×10^{-10} Torr. The Pt(1 1 1) crystal was resistively heated to 1200 K and cooled to 87 K by direct contact of the copper block of the sample holder with liquid-nitrogen. A chromel–alumel, type K thermocouple was spot welded directly to the edge of the crystal. The Pt(1 1 1) surface was cleaned by cycles of Ar^+-ion sputtering with the sample held at 800 K followed by exposure to 1×10^{-7}-Torr of O_2 at 800 K and annealing the crystal at 1200 K for 10 s. The cleanliness and long-range order of the surfaces were checked by AES and LEED.

TPD measurements were made using a UTI 100C quadrupole mass spectrometer in line-of-sight with the sample surface and using a linear heating rate of ~4 K/s. The crystal was located at 2 mm in front of the entrance of a shielded aperture.

IRAS was carried out at a grazing incidence angle of 86° from the surface normal. An Infinity® 60 M FTIR spectrometer and a medium-band, liquid-nitrogen cooled, mercury cadmium telluride (MCT) detector was used for collecting the IR spectra. Typically, spectra were taken at a spectrometer resolution of 4 cm^{-1} and by averaging 1000 scans taken over 8 min. Samples were dosed CO at 87 K and then heated to desorb CO in a controlled fashion to study a range of CO surface coverages. The samples were then allowed to cool down for the acquisition of each spectrum. All of the spectra reported were taken with the sample at a temperature of 87–90 K and ratioed against the clean surface spectrum as a background.

CO (Matheson, 99.5%) was dosed using leak valves. The exposures are given in units of Langmuir (1 L = 10^{-6} Torr s) uncorrected for the dozer enhancement factor and ion gauge sensitivity. Adsorbate coverages in this paper are referenced to the Pt(1 1 1) surface atom density, i.e., $\theta = 1.0$ corresponds to 1.505×10^{15} atoms/cm^{-2}.

The (2×2) and $\sqrt{3}$ surfaces were prepared by evaporating Sn on the clean Pt(1 1 1) crystal surface and subsequently annealing the sample to 1000 K for 10 s. Depending on the initial deposited Sn coverage, the annealed surface exhibited either (2×2) or $(\sqrt{3} \times \sqrt{3})R30^\circ$ LEED pattern [30].

3. Results and discussion

3.1. CO adsorption

TPD spectra of CO adsorption on the Pt(1 1 1) and the two alloy surfaces for saturation coverage are displayed in Fig. 2. These results are in agreement with previous reports [4,33] presenting broad desorption peaks for the three surfaces. Peaks shift to lower temperatures with increasing Sn which indicates that the binding energy of CO on the surface alloys is reduced by a few kcal/mol compared to the Pt(1 1 1) surface. No evidence of dissociative CO desorption was observed on any of the surfaces. A visible shoulder

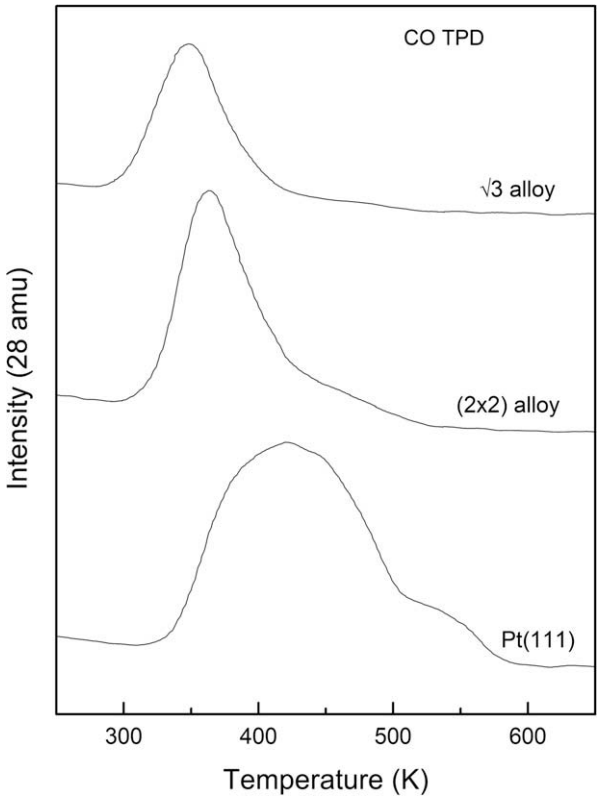

Fig. 2. CO TPD spectra after CO adsorption on Pt(1 1 1) and two ordered Sn/Pt(1 1 1) surface alloys at 100 K.

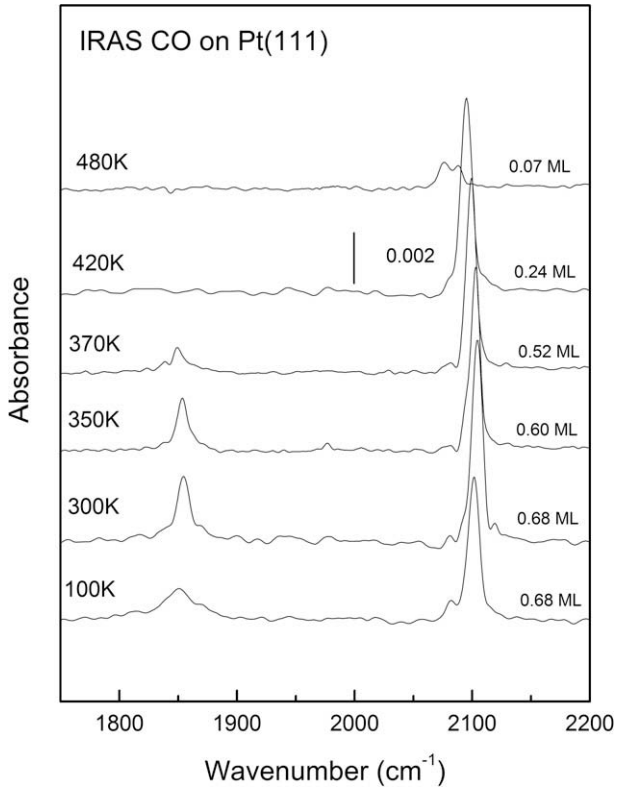

Fig. 3. IRAS spectra obtained for CO adsorbed on Pt(1 1 1) following CO exposure to give saturation monolayer coverage at 90 K and then subsequently heating to different temperatures. All spectra were obtained at 100 K. The indicated CO coverages were obtained from separate TPD experiments carried out under identical conditions.

at higher temperatures for the Pt(1 1 1) surface may be due to a large amount of defects on the original metal surface. The saturation coverages for the Pt(1 1 1), (2×2) and $(\sqrt{3} \times \sqrt{3})$ surfaces were found to be θ_{CO} = 0.68 ML, θ_{CO} = 0.65 ML and θ_{CO} = 0.53 ML, respectively, in accordance with previous studies [4].

3.2. IRAS

CO adsorption on the surface alloys was studied at 90 K by IRAS. Figs. 3–5 display the spectra for Pt(1 1 1), (2×2) alloy and $\sqrt{3}$ alloy surfaces, respectively. Samples were dosed with CO at 87 K and were resistively heated to the indicated temperature. Increasing the temperature before desorption occurs increases the mobility of the molecules allowing them to reorganize and adopt a more stable structure. Thus the Pt(1 1 1) surface was heated to 300 K (Fig. 3), the (2×2) alloy surface was heated to 280 K (Fig. 4) and the $\sqrt{3}$ alloy surface was heated to 270 K (Fig. 5). This results in absorption peaks that sharpen and shift slightly to higher frequencies. On all surfaces we observe a minor coverage dependence of the CO stretching frequency that shift to higher vibrational energies at higher coverages (lower temperatures). These coverage dependent frequency shifts are generally attributed to a combination of neighboring dipole–dipole interactions and electrostatic interactions with the substrate [34,35].

For the Pt(1 1 1) surface, two vibrational bands are observed for saturation coverage at 1855 and 2104 cm^{-1} corresponding to stretching modes of CO adsorbed in twofold bridge and in atop sites, respectively [4,26,36–38]. Fig. 3 shows that the intensity of bridge CO species decreases with reduced CO coverage (increasing the sample temperature). The (2×2) alloy surface displays one absorption peak at 2088 cm^{-1} for saturation coverage (Fig. 4). This peak is assigned to the stretching of atop bonded CO molecule. No peak corresponding to bridge CO species was observed at saturation coverage. At 0.27 ML coverage a peak at 1870 cm^{-1} assigned to bridge bonded CO clearly appears. In contrast, HREELS studies have observed both atop and bridge site CO species at saturation coverage on (2×2) surface alloys [4] and (2×2) Pt_3Sn(1 1 1) bulk alloy surfaces [9]. On the $\sqrt{3}$ alloy surface, only the CO atop bonded stretching band is observed at 2080 cm^{-1} and no bridge bonded peak is observed for any coverage (Fig. 5). This result is also contrary to what has been observed by HREELS [4] in which the bridge site peak is visible for saturation coverage.

There is a notable shift of the CO atop bonded stretching band to lower wavenumber with an increase of surface Sn as depicted in Fig. 6a. Only the Pt(1 1 1) presents a populated bridge site, expressed as the appearance of a peak at 1855 cm^{-1} at this high coverage. Conversely, for low coverages, the bridge sites are populated only for the (2×2) alloy, manifested as the appearance of a peak at ~1870 cm^{-1} in Fig. 6b. Apparently CO never populates bridge sites on the $\sqrt{3}$ surface alloy.

Our measurements of CO bridge site populations at saturation coverage for the three surfaces differ from previous HREELS studies on surface alloys [4] and bulk Pt_3Sn(1 1 1) surfaces [9]. On the Pt(1 1 1) surface, we observe that the intensity ratio of bridge to atop peaks (~0.29) is far lower than those reported by Paffet (~0.43). One could assign this discrepancy to a difference in HREELS and IR selection rules arising from different absorption cross-sections for photons and electrons. Alternatively the observed bridges sites reported by Paffet et al. could be assigned to CO adsorbed at defect sites. The procedures for alloy preparation have improved over the past 10 years and thus the quality of the alloy surfaces may be different. The condition of the alloys reported in this paper was tested by butane TPD studies. The corresponding desorption peaks indicated that the alloys were properly

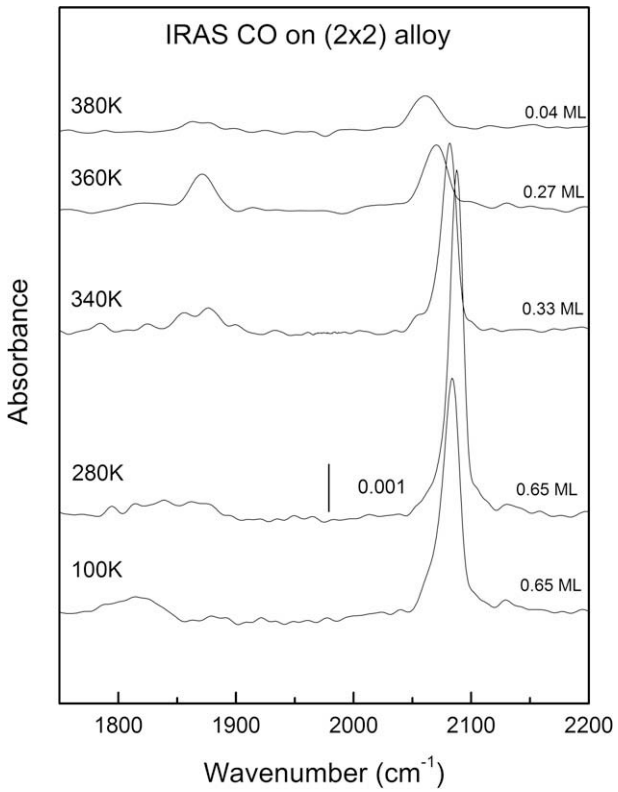

Fig. 4. IRAS spectra for CO adlayers on (2×2) Sn/Pt(1 1 1) surface alloy following a large CO exposure to give saturation monolayer coverage at 90 K and then subsequently heating to different temperatures. All spectra were obtained at 100 K. The indicated CO coverages were obtained from separate TPD experiments carried out under identical conditions.

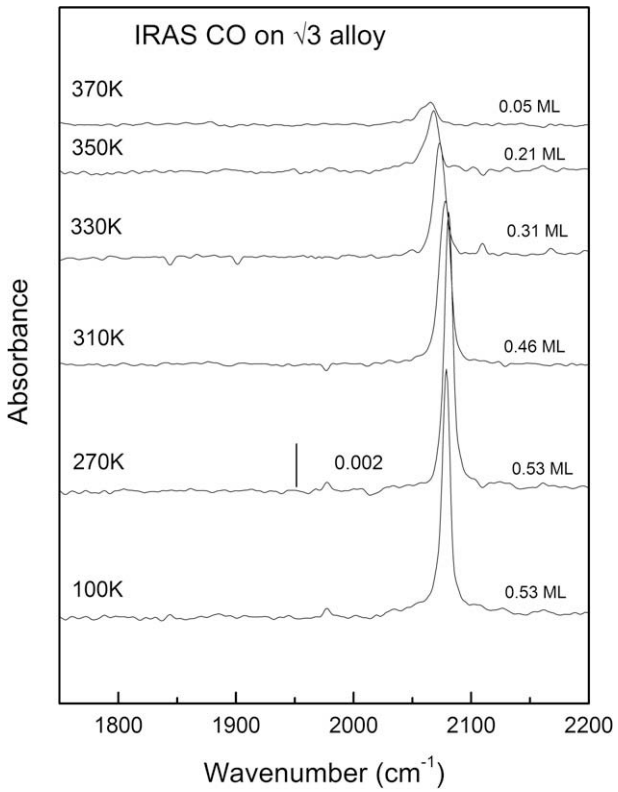

Fig. 5. IRAS spectra for CO adlayers on $(\sqrt{3} \times \sqrt{3})R30°$ Sn/Pt(1 1 1) (2×2) surface alloy following a large CO exposure to give a saturation monolayer coverage at 90 K and then subsequently heating to different temperatures. All spectra were obtained at 100 K. The indicated CO coverages were obtained from separate TPD experiments carried out under identical conditions.

prepared. In a similar study, Xu et al. observed no bridge bonded CO on the ordered $(\sqrt{3} \times \sqrt{3})R30°$ Sn/Ni(1 1 1) surface alloys but did observe bridge bonded CO on disordered alloy surfaces, supporting the hypothesis that the bridge bonded CO can be observed in defective surface alloys [6].

Another contribution the discrepancy between IRAS and HREELS CO population assignments could lie in the reduced number of Pt sites on the alloy surfaces. The number of available Pt binding sites on the (2×2) alloy is reduced by 25% relative to the Pt(1 1 1) surface while the saturation CO coverage on the (2×2) alloy is reduced by ~5%. This "condensed" phase of chemisorbed CO on (2×2) alloys displayed a LEED pattern previously denoted $(2\sqrt{3} \times 2\sqrt{3})R30°$ structure relative to the integral order beams of Pt(1 1 1) at 100 K [4]. Fig. 11 displays a possible real space structure of saturated CO adlayers on the (2×2) alloy that is consistent with our LEED and IRAS studies. The proposed structure has a CO coverage of 8/12 per unit cell ($\theta_{CO} = 0.66$). The ratio of atop to bridge species is 7:1 within this suggested unit cell on the (2×2) alloy relative to the 1:1 for the $c(4 \times 2)$-CO ($\theta_{CO} = 0.5$) and 4:1 for the $c(\sqrt{3} \times 7)$-CO ($\theta_{CO} = 0.71$) [26]. The high ratio of atop to bridge species in the proposed structure along with "intensity" transfer associated with dynamic dipole–dipole coupling could account for the lack of a IRAS peak corresponding to bridge coordinated CO on the saturated (2×2) alloys surface.

CO interaction with Sn/Pt(1 1 1) alloys has been studied electrochemically by Tillmann et al. [39]. Though the particular ordering of the Sn/Pt(1 1 1) bimetallic surface was not reported, there are similarities with the present studies worth noting. In both studies, the addition of Sn provoked a reduction of CO coverages as observed by the reduction of the intensity of the IR absorption peaks. For the bare Pt(1 1 1) surfaces a similar frequency shift to higher wavenumbers with higher CO coverages was observed. The occupation of CO bridge sites was significantly affected by the addition of Sn as indicated by potential dependent changes in frequencies and intensity of the bridge bonded CO.

It is interesting to note that we do not observe CO bonded to threefold hollow sites on the Pt(1 1 1), (2×2) and $(\sqrt{3} \times \sqrt{3})$ surfaces. Electrochemical studies on Pt(1 1 1) and Pt(1 1 1)/Sn bimetallic surfaces show that CO can populate threefold hollow sites on Pt(1 1 1) by tuning the potential (~0 V vs. SCE) but never on the Pt(1 1 1)/Sn bimetallic surface [37,39,40]. CO can also metastably populate threefold hollow sites on the Pt(1 1 1) under UHV conditions and at extremely low temperatures (20–50 K) [36,41]. In the case of the electrochemical systems, excess surface charge associated with low potentials increases electronic transfer from the $d\pi \rightarrow 2\pi^*$ for metal-CO back bonding. This leads to the favoring CO coordination with greater overlap between CO $2\pi^*$ and metal orbital, thus threefold hollow vs. atop CO coordination [38].

One can make simple arguments to account for the absence of CO threefold hollow on alloy surfaces observed in this study. In the case of $\sqrt{3}$ surfaces, there do not exist threefold hollow sites comprised of only Pt atoms. In the case of the (2×2) surface alloy, charge transfer from the Pt 5d to Sn 5p [42] results in reduced overlap between the substrate and CO $2\pi^*$ orbitals. It could be argued that this charge transfer on the (2×2) surface alloy favors CO atop coordination with its greater overlap between 5σ and substrate orbitals.

3.3. High pressure studies

High pressure CO experiments were performed in the same chamber for the three alloy surfaces. IR spectrums were taken both at 300 and 90 K for CO pressures of 0.1, 1 and 10 Torr. Only atop site

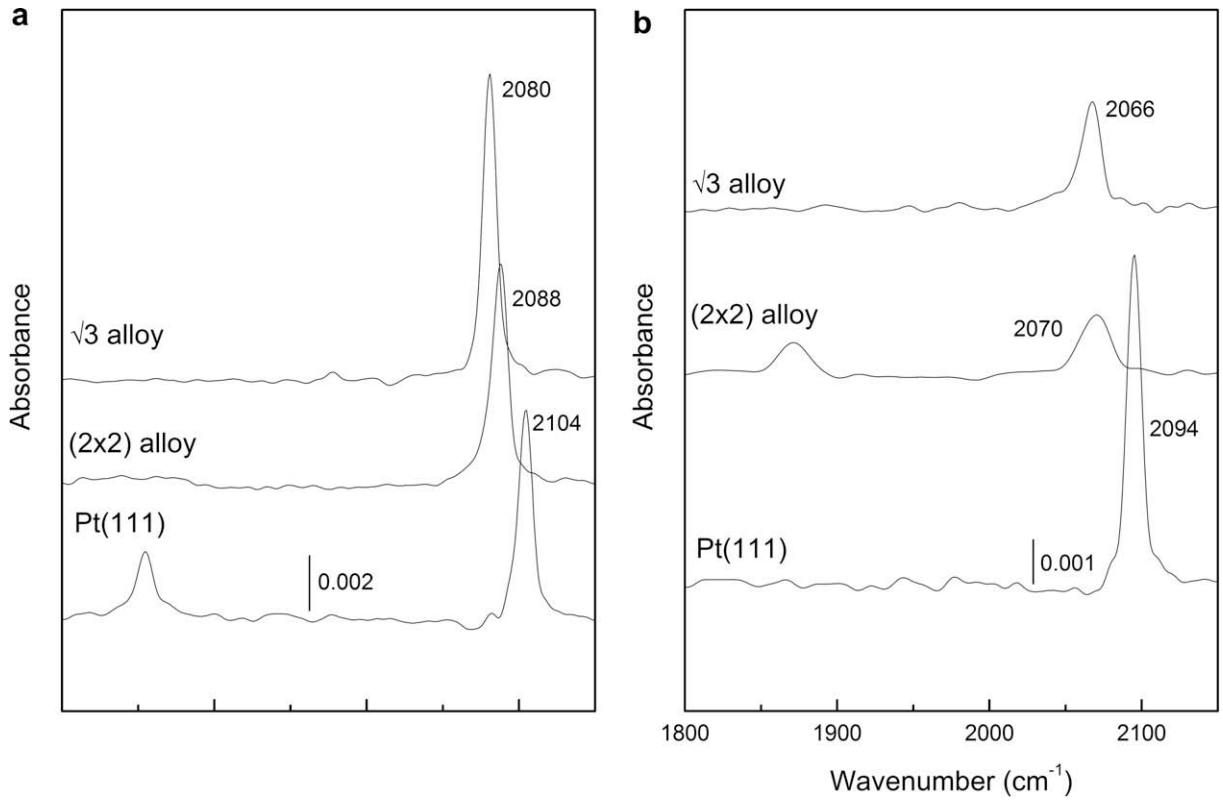

Fig. 6. (a) Comparison of vibrational spectra for CO adlayers at (a) near-monolayer coverages obtained after large CO exposures and annealing to 300 K (0.68 ML), 280 K (0.65 ML) and 270 K (0.53 ML) for Pt(1 1 1), (2 × 2) alloy and $\sqrt{3}$ alloy surfaces, respectively; (b) relatively low coverages obtained after annealing up to 420 K (0.24 ML), 360 K (0.27 ML) and 350 K (0.21 ML) for Pt(1 1 1), (2 × 2) alloy and $\sqrt{3}$ alloy surfaces, respectively.

occupancy was observed for the three surfaces at high pressure as observed in Figs. 7–9 and just a low intensity bump could be assigned to bridge site adsorbed CO at frequencies of ~1850–1890 cm^{-1} for the Pt(1 1 1) surface. At 10 Torr, the gas CO molecules absorption becomes important giving a very high background. The CO gas absorption band frequencies are between 2050 and 2230 cm^{-1}. By comparison to the spectrum taken under UHV conditions at same temperature, it can be seen that frequencies of atop site assigned peaks slightly red shift as pressure increases. It is also noticeable that the intensity of peaks is comparable showing saturation behavior. The absence of peaks at other frequencies indicates that there is no direct CO bonding to Sn sites. Experiments performed at 90 K show the same behavior. Comparison of high pressure IRAS spectra of the three surfaces display similar features as those in UHV conditions, see Fig. 10 contrasted to Fig. 6.

Simple Langmuir isotherm calculations were made in order to test the possibility of CO adsorbing on Sn at high pressures. These calculations are based on the derivation of the Langmuir isotherm that balances the adsorption and desorption rates (R_{ads} and R_{des}, respectively) at equilibrium.

$$\theta = \frac{(bP)^{1/n}}{\left(1 + (bP)^{1/n}\right)} \tag{1}$$

and

$$b = \frac{\sigma}{2\pi mkT} \exp(-\Delta H_{ads}/RT) - \nu N_o^n \tag{2}$$

where θ is the Langmuir definition for coverage, P is pressure, m is molecular mass, k is Boltzmann's constant, T is temperature, σ is a steric factor, ΔH_{ads} is the adsorption enthalpy, N_o is the number of adsorption sites per unit area, R is the gas constant, ν is the Arrhenius factor for desorption, and $n = 1$ for molecular adsorption.

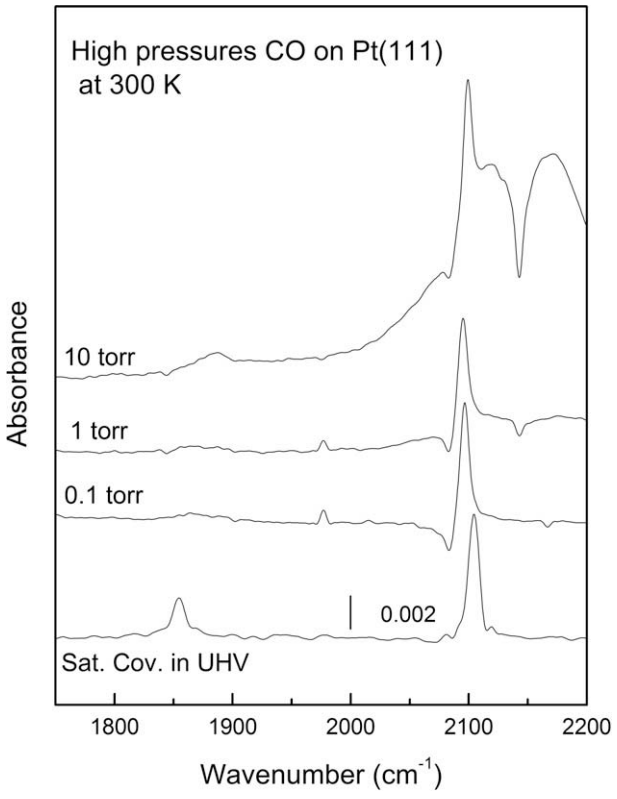

Fig. 7. *In situ* IRAS spectra of a Pt(1 1 1) surface in the presence of high pressures of CO at 300 K. For comparison, the IRAS spectrum of saturation coverage CO on a Pt(1 1 1) under UHV conditions (2×10^{-10} Torr) is shown at the bottom of the figure.

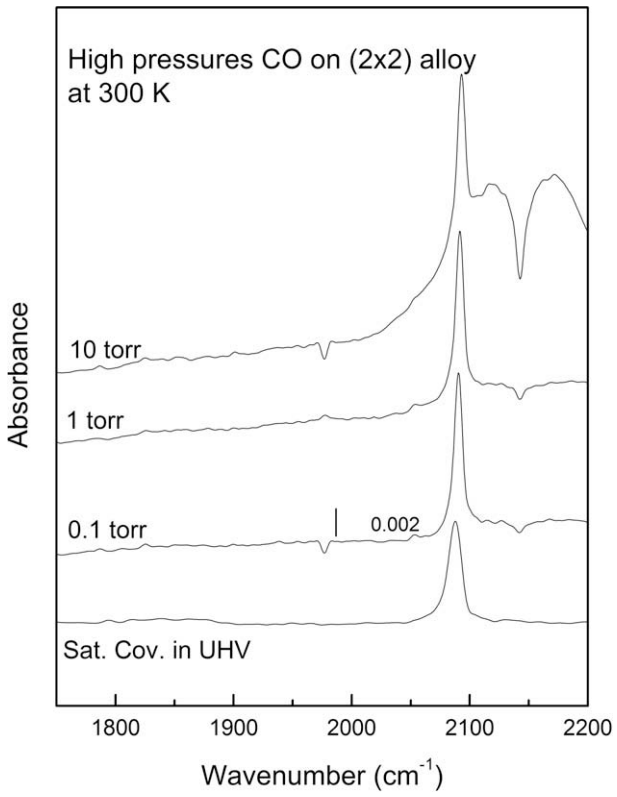

Fig. 8. *In situ* IRAS spectra of a (2×2) alloy surface in the presence of high pressures of CO at 300 K. For comparison, the IRAS spectrum of saturation coverage CO on a Pt(1 1 1) under UHV conditions (2×10^{-10} Torr) is shown at the bottom of the figure.

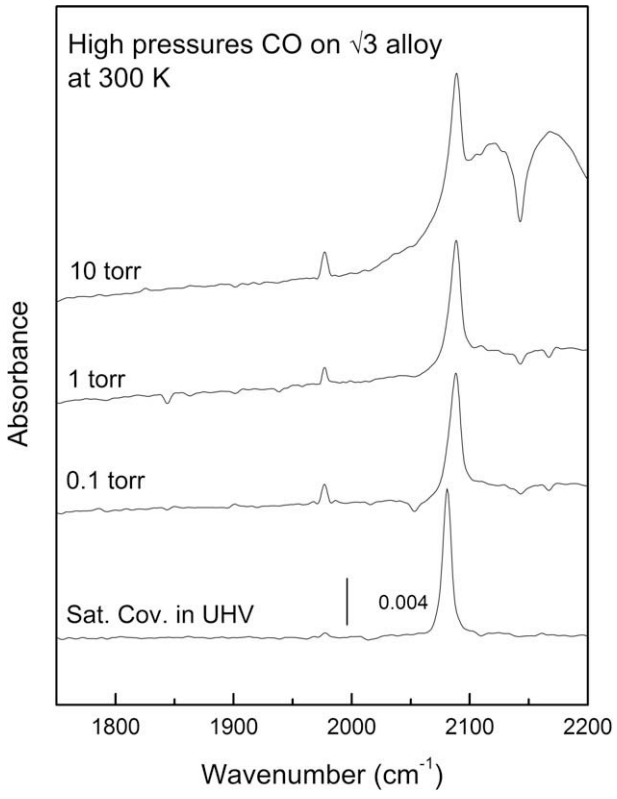

Fig. 9. *In situ* IRAS spectra of a $\sqrt{3}$ alloy surface in the presence of high pressures of CO at 300 K. For comparison, the IRAS spectrum of saturation coverage CO on a Pt(1 1 1) under UHV conditions (2×10^{-10} Torr) is shown at the bottom of the figure.

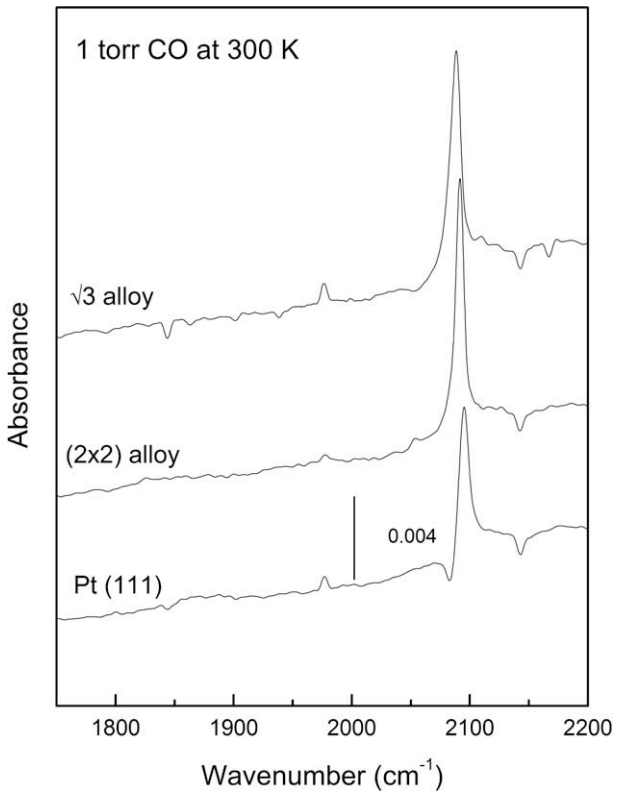

Fig. 10. Comparison of vibrational spectra for high pressure CO at 300 K on Pt(1 1 1), (2×2) alloy and $\sqrt{3}$ alloy surfaces.

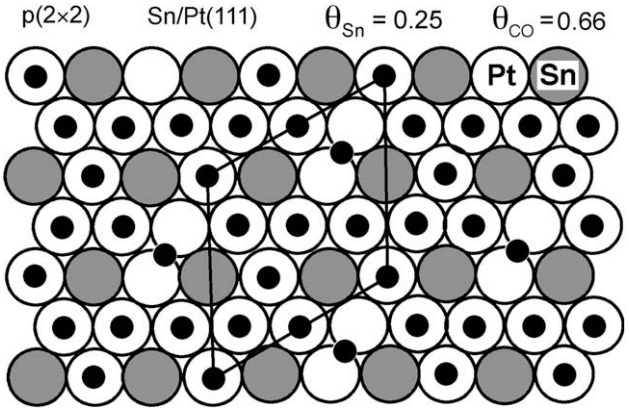

Fig. 11. Proposed real space models of the $(2\sqrt{3} \times 2\sqrt{3})R30^\circ$ CO overlayer for the LEED pattern (2×2) alloy.

These calculations predict that molecules with a ΔH_{ads} of 8 kcal/mol or less will have $\theta \leqslant 0.01$ at 100 K and 10 Torr. Furthermore, molecules with a ΔH_{ads} of 16 kcal/mol or less will have $\theta \leqslant 0.01$ at 200 K and 10 Torr. These values for temperature and pressure correspond to the experimental parameters of our vibrational studies of CO adsorption on Sn/Pt(1 1 1) alloys. We thus conclude that adsorption enthalpy on CO on Sn is less than 8 kcal/mol. It is interesting to note that systems with ΔH_{ads} of 8 kcal/mol at 100 K and 764 Torr are predicted to have a $\theta = 0.26$. High pressure PM-IRRAS studies of CO on bulk $Pt_3Sn(1\,1\,1)$ surfaces at room temperature and 100 Torr observed only the peak corresponding to atop bonded CO on platinum [18].

From the presented IRAS studies and Langmuir isotherm calculations we conclude that there is no direct CO bonding to Sn sites. This conclusion is supported by several CO adsorption studies on

Sn. Theoretical calculations, both DFT calculations for Pt_3Sn [43] and relativistic density-functional self-consistent field method on Pt–Sn clusters [44], find that CO adsorbed on Pt but not on Sn. Studies of silica supported Sn show no CO adsorption at 773 K and 30 Torr [45]. Correlation between chemical titration of CO on Pt_3Sn single crystals and low energy ion scattering (LEIS) also suggests selective adsorption of CO to Pt sites [46]. Finally, *in situ* FTIR electrochemical studies on Pt_3Sn and Pt–Sn electrodes also report no CO adsorption on Sn [39,40].

4. Conclusion

Two ordered Sn/Pt(1 1 1) surface alloys with $\theta_{Sn} = 0.25$ and 0.33 ML were prepared by vapor deposition of Sn on Pt(1 1 1) surface in a UHV chamber. CO adsorption on these surfaces and on bare Pt(1 1 1) was studied by TPD and IRAS. Different occupations of sites were observed for the three surfaces with the adsorption on bridge site the most sensitive to the presence of Sn. Also, the vibrational frequency of atop bonded CO is affected by the presence of Sn, being shifted to lower energies as the amount of Sn increases. Coverage dependence of the vibrational frequencies of adsorbed CO was evident, shifting to higher energies as the coverage increase. High pressures IRAS experiments at 300 K show no bridge bonded CO on any of the surfaces and no CO adsorbed on pure Sn sites.

Acknowledgements

This material is based upon work supported by the National Science Foundation grant 0616644. AH acknowledges a fellowship from MERCK/United Negro College Fund.

References

[1] J.H. Sinfelt, Bimetallic Catalysis: Discoveries, Concepts, and Applications, Wiley, New York, 1983.
[2] J.A. Rodriguez, Surface Science Reports 24 (7–8) (1996) 225.
[3] M.T.M. Koper, Surface Science 548 (1–3) (2004) 1.
[4] M.T. Paffett, S.C. Gebhard, R.G. Windham, B.E. Koel, Journal of Physical Chemistry 94 (1990) 6831.
[5] C. Xu, B.E. Koel, Surface Science 304 (3) (1994) L505.
[6] C. Xu, B.E. Koel, Surface Science 327 (1995) 38.
[7] K. Fukutani, T.T. Magkoev, Y. Murata, K. Terakura, Surface Science 363 (1–3) (1996) 185.
[8] H. von Schenck, E. Janin, O. Tjernberg, M. Svensson, M. Gothelid, Surface Science 526 (1–2) (2003) 184.
[9] C. Dupont, D. Loffreda, F. Delbecq, Y. Jugnet, Journal of Physical Chemistry C 111 (24) (2007) 8524.
[10] M. Kinne, T. Fuhrmann, C.M. Whelan, J.F. Zhu, J. Pantforder, M. Probst, G. Held, R. Denecke, H.P. Steinruck, Journal of Chemical Physics 117 (23) (2002) 10852.
[11] R.M. Watwe, R.D. Cortright, M. Mavrikakis, J.K. Norskov, J.A. Dumesic, Journal of Chemical Physics 114 (10) (2001) 4663.
[12] Y.M. Jin, A.K. Datye, E. Rightor, R. Gulotty, W. Waterman, M. Smith, M. Holbrook, J. Maj, J. Blackson, Journal of Catalysis 203 (2) (2001) 292.
[13] N.M. Markovic, P.N. Ross, Surface Science Reports 45 (4–6) (2002) 121.
[14] X.C. Su, P.S. Cremer, Y.R. Shen, G.A. Somorjai, Physical Review Letters 77 (18) (1996) 3858.
[15] G. Rupprechter, T. Dellwig, H. Unterhalt, H.J. Freund, Journal of Physical Chemistry B 105 (18) (2001) 3797.
[16] G. Rupprechter, H. Unterhalt, M. Morkel, P. Galletto, T. Dellwig, H.J. Freund, Vacuum 71 (1–2) (2003) 83.
[17] M. Sushchikh, J. Lauterbach, W.H. Weinberg, Surface Science 393 (1–3) (1997) 135.
[18] C. Dupont, D. Loffreda, F. Delbecq, F. Aires, E. Ehret, Y. Jugnet, Journal of Physical Chemistry C 112 (29) (2008) 10862.
[19] M. Batzill, D.E. Beck, B.E. Koel, Surface Science 466 (2000) L821.
[20] R. Bouwman, P. Biloen, Surface Science 41 (2) (1974) 348.
[21] S.H. Overbury, D.R. Mullins, M.T. Paffett, B.E. Koel, Surface Science 254 (1–3) (1991) 45.
[22] H. Hopster, H. Ibach, Surface Science 77 (1) (1978) 109.
[23] H. Steininger, S. Lehwald, H. Ibach, Surface Science 123 (2–3) (1982) 264.
[24] R.A. Olsen, P.H.T. Philipsen, E.J. Baerends, Journal of Chemical Physics 119 (8) (2003) 4522.
[25] G. Kresse, A. Gil, P. Sautet, Physical Review B 68 (7) (2003).
[26] B.N.J. Persson, M. Tushaus, A.M. Bradshaw, Journal of Chemical Physics 92 (8) (1990) 5034.
[27] M.A. Gulmen, A. Sumer, A.E. Aksoylu, Surface Science 600 (21) (2006) 4909.
[28] V. Stamenkovic, M. Arenz, B.B. Blizanac, K.J.J. Mayrhofer, P.N. Ross, N.M. Markovic, Surface Science 576 (1–3) (2005) 145.
[29] C. Creemers, P. Deurinck, S. Helfensteyn, J. Luyten, Applied Surface Science 219 (1–2) (2003) 11.
[30] M.T. Paffett, R.G. Windham, Surface Science 208 (1–2) (1989) 34.
[31] B.N.J. Persson, R. Ryberg, Physical Review B 40 (15) (1989) 10273.
[32] B.N.J. Persson, R. Ryberg, Physical Review B 24 (12) (1981) 6954.
[33] C. Xu, B.E. Koel, Surface Science 310 (1–3) (1994) 198.
[34] A. Crossley, D.A. King, Surface Science 95 (1) (1980) 131.
[35] M.W. Severson, C. Stuhlmann, I. Villegas, M.J. Weaver, Journal of Chemical Physics 103 (22) (1995) 9832.
[36] J.V. Nekrylova, I. Harrison, Chemical Physics 205 (1–2) (1996) 37.
[37] B.E. Hayden, M.E. Rendall, O. South, Journal of the American Chemical Society 125 (25) (2003) 7738.
[38] I. Villegas, M.J. Weaver, Journal of Chemical Physics 101 (2) (1994) 1648.
[39] S. Tillmann, G. Samjeske, K.A. Friedrich, H. Baltruschat, Electrochimica Acta 49 (1) (2003) 73.
[40] V.R. Stamenkovic, M. Arenz, C.A. Lucas, M.E. Gallagher, P.N. Ross, N.M. Markovic, Journal of the American Chemical Society 125 (9) (2003) 2736.
[41] J.V. Nekrylova, C. French, A.N. Artsyukhovich, V.A. Ukraintsev, I. Harrison, Surface Science 295 (1–2) (1993) L987.
[42] E. Shustorovich, R.C. Baetzold, Science 227 (4689) (1985) 876.
[43] T.E. Shubina, M.T.M. Koper, Electrochimica Acta 47 (22–23) (2002) 3621.
[44] M.S. Liao, C.R. Cabrera, Y. Ishikawa, Surface Science 445 (2–3) (2000) 267.
[45] B.A. Riguetto, J.M.C. Bueno, L. Petrov, C.M.P. Marques, Spectrochimica Acta A 59 (2003) 2141.
[46] A.H. Haner, P.N. Ross, U. Bardi, A. Atrei, Journal of Vacuum Science and Technology A (Vacuum, Surfaces, and Films) 10 (4) (1992) 2718.